ESD-TR-87-093

Technical Report
795

On the Design of Suboptimal Matched Filters for Three-Dimensional Moving Target Detection

Y. Chen

20 November 1987

Lincoln Laboratory
MASSACHUSETTS INSTITUTE OF TECHNOLOGY
LEXINGTON, MASSACHUSETTS

**Prepared for the Department of the Air Force
under Electronic Systems Division Contract F19628-86-C-0002.**

Approved for public release; distribution unlimited.

ADA188354

The work reported in this document was performed at Lincoln Laboratory, a center for research operated by Massachusetts Institute of Technology. This work was sponsored by the Department of the Air Force under Contract F19628-86-C-0002.

This report may be reproduced to satisfy needs of U.S. Government agencies.

The views and conclusions contained in this document are those of the contractor and should not be interpreted as necessarily representing the official policies, either expressed or implied, of the United States Government.

The ESD Public Affairs Office has reviewed this report, and it is releasable to the National Technical Information Service, where it will be available to the general public, including foreign nationals.

This technical report has been reviewed and is approved for publication.

FOR THE COMMANDER

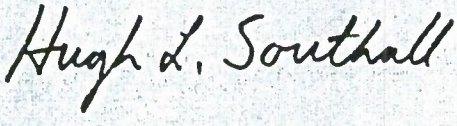

Hugh L. Southall, Lt. Col., USAF
Chief, ESD Lincoln Laboratory Project Office

Non-Lincoln Recipients

PLEASE DO NOT RETURN

Permission is given to destroy this document when it is no longer needed.

MASSACHUSETTS INSTITUTE OF TECHNOLOGY
LINCOLN LABORATORY

ON THE DESIGN OF SUBOPTIMAL MATCHED FILTERS FOR THREE-DIMENSIONAL MOVING TARGET DETECTION

Y. CHEN
Group 27

TECHNICAL REPORT 795

20 NOVEMBER 1987

Approved for public release; distribution unlimited.

LEXINGTON MASSACHUSETTS

ABSTRACT

The optimal detection of a three-dimensional moving target calls for the classical technique of matched filtering. If a target is modeled as a moving point source with unknown velocity, then the velocity alone determines the shape of the observed signal. Thus, target velocity is a parameter that completely characterizes the matched filter. We will designate these types of matched filters to be the assumed velocity filters (AVFs) to emphasize the velocity parameter.

Like most matched filtering techniques where the signal parameters range in a continuum, the AVF must be implemented suboptimally by quantizing the velocity space. In this report we will use a loss factor that measures the average loss of signal-to-noise ratio (SNR) at the output of the matched filter due to mismatch of filter parameters. The loss factor can be used as a criterion for partitioning the velocity space. We will show that, with a fixed loss factor, the number of filters required for coverage increases *linearly* as the span of the two-dimensional velocity space increases quadratically. The rate of increase is further reduced when the loss factor is made proportional to expected target angular speed.

CONTENTS

LIST OF ILLUSTRATIONS

ON THE DESIGN OF SUBOPTIMAL MATCHED FILTERS FOR THREE-DIMENSIONAL MOVING TARGET DETECTION

1 INTRODUCTION

A point target at location $\underline{x}$ traveling at velocity $\underline{v}$ (see *) makes a streak on the focal plane of a telescope. The optimal detection of the three-dimensional target streak calls for the classical technique of matched filtering.[1-3] Assume that the focal plane consists of an array of solid-state photodetectors such as the charge-coupled devices(CCDs). Then we can model the image received at the m-n*th* photodetector cell, denoted by $r_{mn}(\underline{x}, \underline{v})$, to be the sum of three independent Poisson processes — the photoelectrons produced because of the target image, the photoelectrons produced becaused of the sky background noise, and the electrons produced by the photodetector noise (e.g., the CCD dark-current)† The $r_{mn}(\underline{x}, \underline{v})$ itself is therefore a Poisson process (due to the reproductive property of the Poisson distribution) with the average number of electrons given by $\lambda_s s_{mn}(\underline{x}, \underline{v}) + \lambda_0$, where λ_s is the electron rate per unit intensity of the target signal, λ_0 is the electron rate of the combined noise, and s_{mn} is the target signal.

Using the Poisson distributions, the likelihood ratio is found to be

---

* Unless stated otherwise, all velocities refer to angular velocities measured in pixels per frame time.

† Notably absent is readout circuit noise, which is considered negligible due to recent engineering improvements.

$$\Lambda = \Pi_{m,n} \frac{(\lambda_s s_{mn} + \lambda_0)^{r_{mn}} \exp[-(\lambda_s s_{mn} + \lambda_0)]}{\lambda_0^{r_{mn}} \exp(-\lambda_0)}$$
$$= \Pi_{m,n} \left(1 + \frac{\lambda_s s_{mn}}{\lambda_0}\right)^{r_{mn}} \exp(-\lambda_s s_{mn}) \quad . \tag{1}$$

Taking logarithms of both sides, we get the log likelihood ratio

$$\ln \Lambda = \sum_{mn} r_{mn} \ln \left(1 + \frac{\lambda_s s_{mn}}{\lambda_0}\right) - \sum_{mn} \lambda_s s_{mn} \quad . \tag{2}$$

Assume that $\lambda_s s_{mn} \ll \lambda_0$. Then

$$\ln \left(1 + \frac{\lambda_s s_{mn}}{\lambda_0}\right) \approx \frac{\lambda_s s_{mn}}{\lambda_0} \quad . \tag{3}$$

Substituting Equation (3) into (2) yields

$$\ln \Lambda = \frac{\lambda_s}{\lambda_0} \sum_{mn} (r_{mn} - \lambda_0) s_{mn} \quad . \tag{4}$$

Equation (4) provides a formula for the matched-filter detection of the stressing case of a weak target streak.[3] For stronger targets, detection [Equation (4)] is suboptimal, although the increased signal strength has more than compensated for that.

In Equation (4), the quantity $\sum_{mn} \lambda_0 s_{mn}$ is not data dependent, and is usually combined with the detection threshold. In the following work, however, we have found it useful to retain this term.

Let us assume that the focal plane is sufficiently large and that the detectors are sufficiently small, and that we can replace Equation (4) by an integral

$$\ln \Lambda = \frac{\lambda_s}{\lambda_0} \int_{R^2} [r(\underline{x}) - \lambda_0] s(\underline{x}) d\underline{x} \quad . \tag{5}$$

In Equation (5), $\underline{x}$ is a two-dimensional vector and R^2 is the second Cartesian product of the real line. We resort to the integral form because the mathematics involved is somewhat simpler.

In the case of N statistically independent image frames with frame period T, Equation (5) can be modified as

$$\ln \Lambda = \frac{\lambda_s}{\lambda_0} \sum_{i=0}^{N} \int_{R^2} [r_i(\underline{x}) - \lambda_0] s(\underline{x} - i\underline{v}_F T) d\underline{x} \tag{6}$$

where we shift the matched filter by an assumed velocity $\underline{v}_F$ (the filter velocity), correlate it with the corresponding image frame, and then sum the correlations computed from the individual frames.

Let $\underline{v}_T$ be the target velocity. Taking the expected value of Equation (6) and using the mean of the observation

$$E[r_i(\underline{x})] = \lambda_s s(\underline{x} - i\underline{v}_T T) + \lambda_0 \tag{7}$$

yields

$$\begin{aligned} E[\ln \Lambda] &= \frac{\lambda_s^2}{\lambda_0} \sum_{i=0}^{N} \int_{R^2} s(\underline{x} - i\underline{v}_T T) s(\underline{x} - i\underline{v}_F T) d\underline{x} \\ &= \frac{\lambda_s^2}{\lambda_0} \sum_{i=0}^{N} \int_{R^2} s(\underline{x} - i(\underline{v}_T - \underline{v}_F) T) s(\underline{x}) d\underline{x} \\ &= \frac{\lambda_s^2}{\lambda_0} \sum_{i=0}^{N} R(i(\underline{v}_T - \underline{v}_F) T) \end{aligned} \tag{8}$$

namely, the autocorrelation of the target signal. Obviously Equation (8) is maximized when $\underline{v}_F = \underline{v}_T$. The result has shown that a maximum likelihood estimator would choose, from all possible velocities, the $\underline{v}_F$ that maximizes Equation (6), i.e.,

$$\hat{\underline{v}}_T = \max_{\underline{v}_F} \sum_{i=0}^{N} \int_{R^2} [r_i(\underline{x}) - \lambda_0] s(\underline{x} - i\underline{v}_F T) d\underline{x} \quad . \tag{9}$$

Notice that the formulation allows us to match filter a random signal by its conditional mean.

2 THE DESIGN OF THE ONE-DIMENSIONAL AVF

We now investigate the output SNR of the matched filters when the assumed velocity $\underline{v}_F$ deviates from the target velocity $\underline{v}_T$ ($\underline{v}_F \neq \underline{v}_T$). We start from the one-dimensional case because it is both simple and enlightening. We will divide the discussion of one-dimensional assumed velocity filters (AVFs) into two parts; in the first, we assume a rectangular-shaped target signal, and in the second, a Gaussian-shaped target signal. The two results share similar characteristics. Therefore, owing to its mathematical tractability, we will apply the Gaussian approximation to the design of the two-dimensional AVF in the next section.

2.1 THE RECTANGULAR-SHAPED SIGNAL

Suppose v_F is mismatched to v_T ($v_F \neq v_T$). By interchanging the summation and the integral in Equation (6) and by changing a variable, we obtain the equivalent expression

$$\ln \Lambda = \frac{\lambda_s}{\lambda_0} \int_R \left\{ \sum_{i=0}^{N} [r_i(x + iv_F T) - \lambda_0] \right\} s(x) dx \quad . \tag{10}$$

The equation suggests that we remove the mean of the noise from each image frame, stack the frames according to the filter velocity v_F, and then correlate the stacked frame with the filter signal. In Figure 1 we have plotted the means of three frames of images, and we have shown that when v_F is mismatched to v_T, the mean of the stacked signal will have the shape of a wedding cake. A loss of SNR ratio is thus incurred when the stacked signal is correlated with the original rectangular signal.

Let the stacked signal be denoted by $y(x)$. Its mean, $\overline{y}(x)$, can be represented by

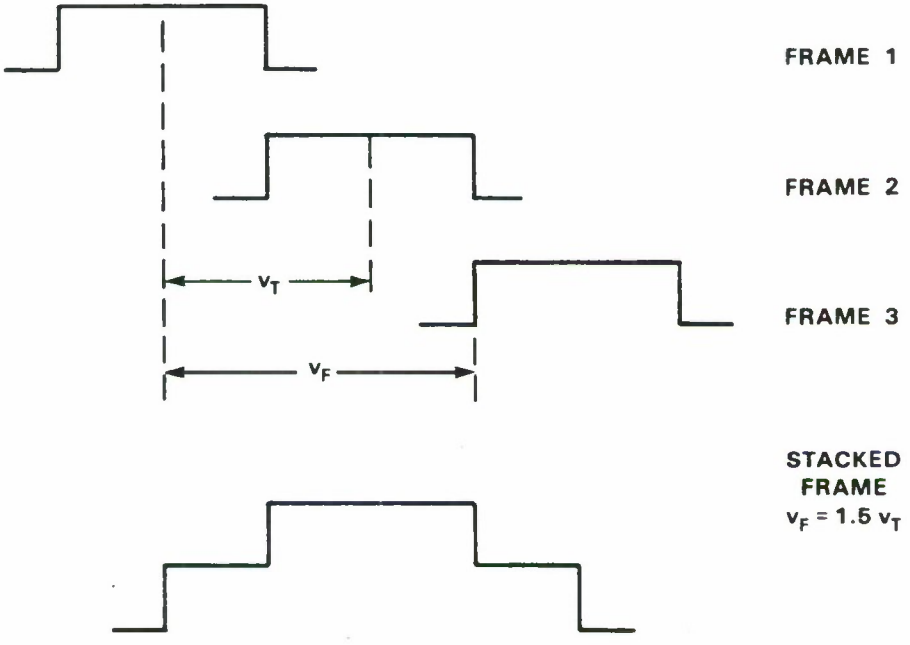

Figure 1. AVF with mismatched velocities.

$$\overline{y}(x) = \lambda_s \sum_{i=0}^{N} s(x - iv_T T + iv_F T) = \lambda_s \sum_{i=0}^{N} s(x + i\Delta v T) \tag{11}$$

where $\Delta v \equiv v_F - v_T$.

Now, for convenience of mathematical manipulation we assume that T is sufficiently small and N is sufficiently large such that the summation in Equation (11) can be replaced by an integral. Then

$$\overline{y}(x) = \lambda_s \int_{-NT/2}^{NT/2} s(x + \Delta vt)dt = \lambda_s \int_R w(t)s(x + \Delta vt)dt \tag{12}$$

where R is the real line and $w(t)$ is a rectangular weighting function defined to be

$$w(t) = \text{rect}\left(\frac{t}{NT}\right) \equiv \begin{cases} 1\,, & |t| < NT/2 \\ 0\,, & |t| > NT/2 \end{cases} \quad . \tag{13}$$

According to Equation (10) we will correlate $\overline{y}(x)$ with a filter signal, which we will refer to as $s_F(x)$. We let the target signal $s(x)$ and the filter signal $s_F(x)$ be rectangular with lengths $v_T T$ and $v_F T$, that is,

$$s(x) = \text{rect}\left(\frac{x}{v_T T}\right) \equiv \begin{cases} 1\,, & |x| < v_T T/2 \\ 0\,, & |x| > v_T T/2 \end{cases} \tag{14}$$

$$s_F(x) = \text{rect}\left(\frac{x}{v_F T}\right) \equiv \begin{cases} 1\,, & |x| < v_F T/2 \\ 0\,, & |x| > v_F T/2 \end{cases} \quad . \tag{15}$$

The mean matched-filter output, denoted by $\overline{S}_{mf}$, is given by

$$\begin{aligned} \overline{S}_{mf} &= \lambda_s \int_R \int_R w(t)s(x + \Delta vt)s_F(x)dx\,dt \\ &= \lambda_s \int_R w(t)R_{s,s_F}(\Delta vt)dt \\ &= \frac{\lambda_s}{\Delta v} \int_R \text{rect}\left(\frac{x}{N\Delta vT}\right) R_{s,s_F}(x)dx \quad . \end{aligned} \tag{16}$$

The third equality in Equation (16) is due to the change of variable $x = \Delta vt$. $R_{s,s_F}(x)$ is the cross correlation of the target and filter signals, pictorially depicted in Figure 2. The rectangular window function $w(x/N\Delta vT)$ is also plotted in Figure 2 in dashed lines.

To evaluate Equation (16), we need to find the area under the trapezoid and enclosed in the window boundaries, shown in Figure 2 as a shaded area. We assume, without loss of generality, that $\Delta v \geq 0$. Furthermore, we assume that

$$\frac{(N-1)\Delta vT}{2} \leq v_T T \quad . \tag{17}$$

The inequality [Equation (17)] imposes the constraint that the temporal window is short enough such that the shifted target images remain mutually correlated. In Figure 2, we see that Equation (17) requires that the window boundaries be enclosed in the trapezoid. Under these assumptions, it can be shown that the filter velocity satisfies

$$v_T \leq v_F \leq \frac{N+1}{N-1} v_T \tag{18}$$

and that the mean-filter output signal is equal to

$$\overline{S}_{mf} = \lambda_s \left[N v_T - \frac{(N-1)^2 \Delta v}{4} \right] T^2 \quad . \tag{19}$$

Of equal interest is the noise variance at the matched-filter output. It is

$$\begin{aligned} \sigma^2_{0,mf} &= \iiiint w(\eta) n(x + v_F\eta, \eta) s_F(x) w(\xi) n(y + v_F\xi, \xi) s_F(y) dx\, dy\, d\eta\, d\xi \\ &= \lambda_0 \int w^2(\eta) d\eta \int s_F^2(\xi) d\xi \\ &= \lambda_0 N v_F T^2 \quad . \end{aligned} \tag{20}$$

The ratio of the square of the mean filter output signal and the noise variance is the SNR at the output of the matched filter. We denote it by SNR_{out}. Then

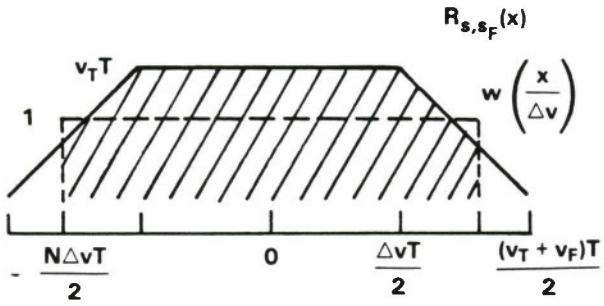

88409-2

Figure 2. Cross correlation function.

$$
\begin{aligned}
\mathrm{SNR}_{out} &= \frac{\overline{S}_{mf}^2}{\sigma_{0,mf}^2} \\
&= \frac{\lambda_s^2[Nv_T - (N-1)^2\Delta v/4]^2T^2}{\lambda_0 N v_F} \\
&= \mathrm{SNR}_{in}\frac{Nv_T^2}{v_F}\left[1 - \frac{(N-1)^2\Delta v}{4Nv_T}\right]^2 T^2
\end{aligned} \tag{21}
$$

where SNR_{in}, the SNR prior to the matched filter, is defined as the square of the mean of the signal divided by the variance of the noise, *viz.*

$$
\mathrm{SNR}_{in} = \frac{\lambda_s^2}{\lambda_0} \quad . \tag{22}
$$

Dividing both sides of Equation (21) by SNR_{in} yields

$$
\frac{\mathrm{SNR}_{out}}{\mathrm{SNR}_{in}} = \frac{Nv_T^2}{v_F}\left[1 - \frac{(N-1)^2\Delta v}{4Nv_T}\right]^2 T^2 \quad . \tag{23}
$$

If the filter is precisely matched to the signal ($\Delta v = 0$), Equation (23) is reduced to

$$
\left.\frac{\mathrm{SNR}_{out}}{\mathrm{SNR}_{in}}\right|_{\Delta v=0} = Nv_T T^2 \quad . \tag{24}
$$

This is the maximum gain in SNR that the matched filter is able to achieve. Substituting Equation (24) back to (23) yields

$$
\frac{\mathrm{SNR}_{out}}{\mathrm{SNR}_{in}} = \left.\frac{\mathrm{SNR}_{out}}{\mathrm{SNR}_{in}}\right|_{\Delta v=0} \frac{v_T}{v_F}\left[1 - \frac{(N-1)^2\Delta v}{4Nv_T}\right]^2 \quad . \tag{25}
$$

Equation (25) describes the average loss of SNR due to velocity mismatch. In the following, we will show that Equation (25) can be used to design the matched filters such that the average SNR loss is no greater than a prescribed loss factor ρ where

$$
\rho \equiv \frac{v_T}{v_F}\left[1 - \frac{(N-1)^2\Delta v}{4Nv_T}\right]^2 \quad . \tag{26}
$$

Let χ be v_F/v_T, α be $(N-1)^2/4N$, and β be $(N+1)^2/4N$. Equation (26) can be rewritten as a quadratic equation in χ

$$\alpha^2\chi^2 - (2\alpha\beta + \rho)\chi + \beta^2 = 0 \quad . \tag{27}$$

Equation (27) has a solution

$$\chi \equiv \frac{v_F}{v_T} = \frac{1}{2\alpha^2}\left(2\alpha\beta + \rho - \sqrt{4\alpha\beta\rho + \rho^2}\right) \tag{28}$$

that satisfies the constraint [see Equation (18)]. This solution gives the largest v_F that satisfies the given ρ. To find the smallest v_F that satisfies the same ρ, one simply interchanges the roles of the target and filter signals in Equation (26). The minimum ratio v_F/v_T is equal to $1/\chi$, as defined in Equation (28).

The design of the suboptimal AVF amounts to using the relationship in Equation (28) to partition the velocity space such that the incurred average loss in filter output SNR is no larger than ρ. Two useful plots are given in Figures 3 and 4. In Figure 3 we have plotted Equation (28) for a set of frame numbers. For example, if $N = 10$ then the maximum v_F that satisfies $\rho = 0.5$ (or 3-dB loss) is $v_F = 1.124v_T$, as indicated in Figure 3 by an open circle. The minimum v_F is given by $v_F = 0.89v_T$.

A useful property that has surfaced from the derivation is that the maximum (as well as the minimum) v_F that satisfies a given ρ is proportional to v_T. That is, the spacing between filter velocities increases as the expected target velocity increases. Therefore, a relatively fewer number of filters is needed to detect higher speed targets than that needed for lower speed targets. This is demonstrated in Figure 4, where we have plotted the numbers of filters required for three velocity ranges (see *, page 1 for unit of velocity): 1 to 50, 1 to 100, and 1 to 200. The number of frames is 10. For example, at 3-dB loss, Figure 4

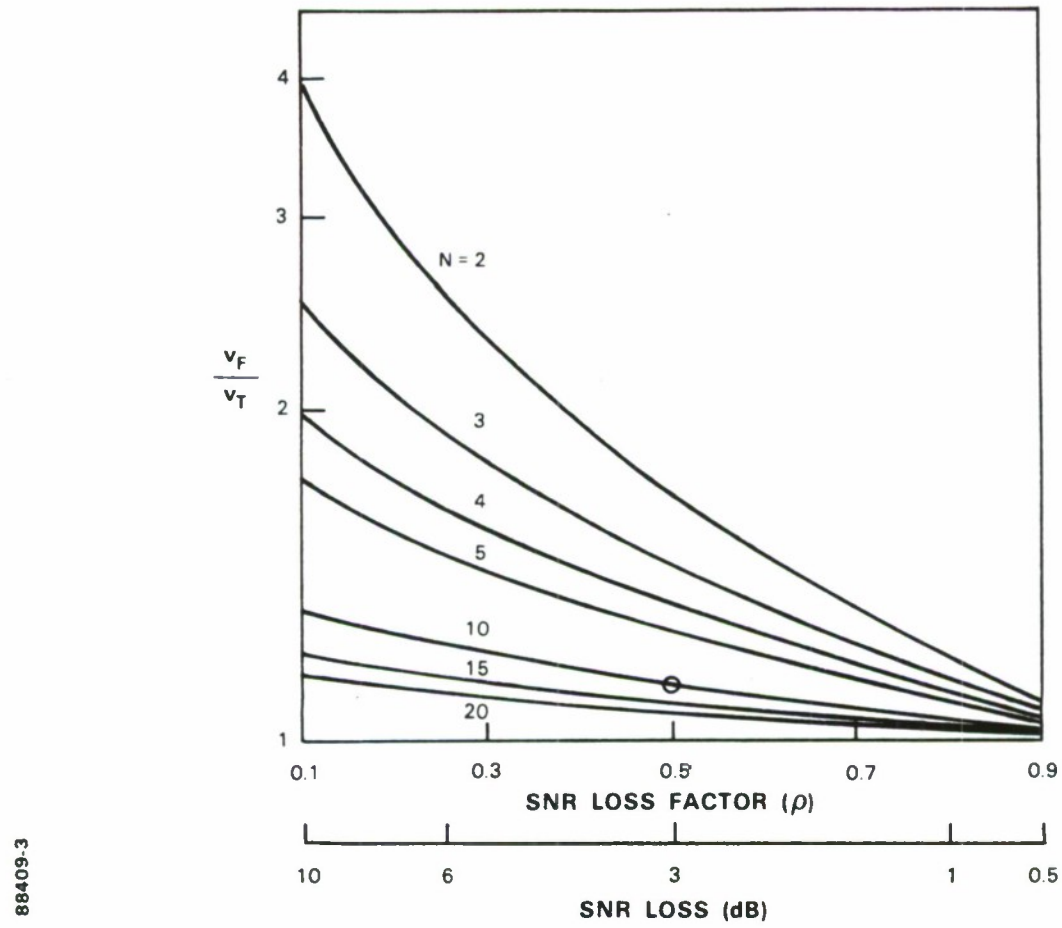

Figure 3. v_F/v_T – rectangular signal.

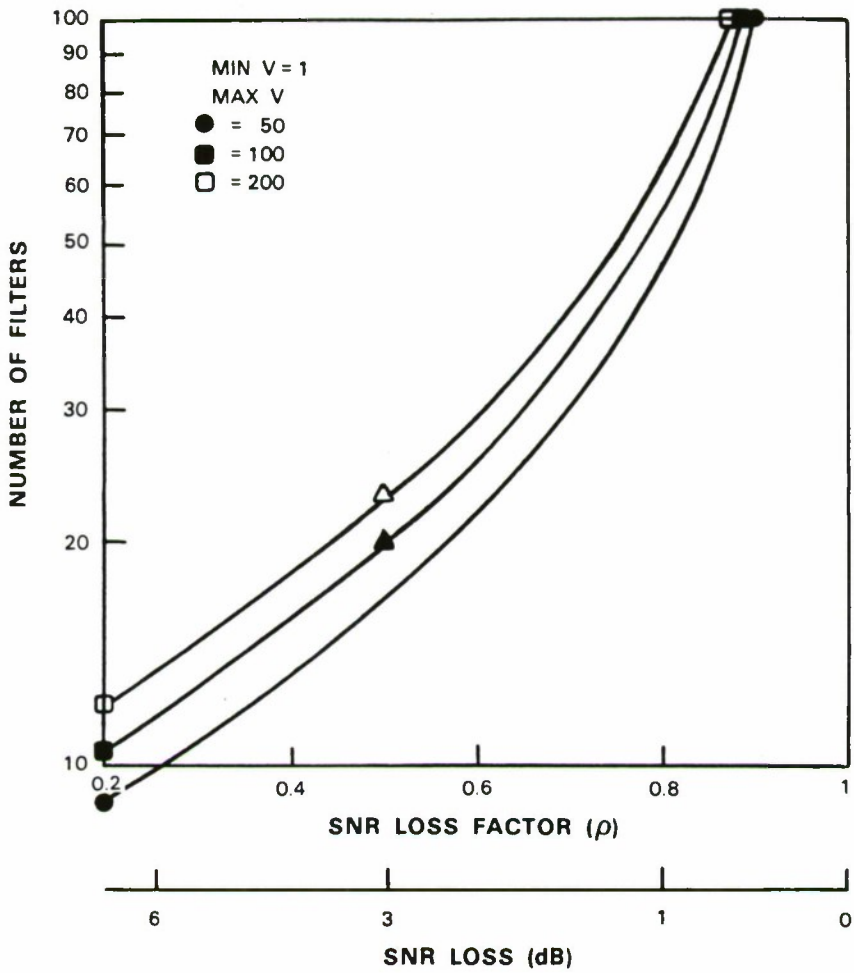

Figure 4. Number of filters required – rectangular signal.

shows that only 22 filters are needed to cover the velocity range 1 to 200 (indicated by an open triangle), but 20 of the 22 filters are used to cover the range 1 to 100 (indicated by a filled triangle). The property is particularly useful when we get to the problem of designing two-dimensional AVF.

2.2 THE GAUSSIAN-SHAPED SIGNAL

In anticipation of the two-dimensional case, we also chose to analyze one-dimensional AVF by using Gaussian approximations. Let

$$s(x) = \sqrt{\frac{6}{\pi}} \exp\left(-\frac{x^2}{2\sigma_T^2}\right) \tag{29}$$

$$s_F(x) = \sqrt{\frac{6}{\pi}} \exp\left(-\frac{x^2}{2\sigma_F^2}\right) \tag{30}$$

$$w(t) = \sqrt{\frac{6}{\pi}} \exp\left(-\frac{t^2}{2\sigma_w^2}\right) \tag{31}$$

where

$$\sigma_T^2 = \frac{(v_T T)^2}{12} \tag{32}$$

$$\sigma_F^2 = \frac{(v_F T)^2}{12} \tag{33}$$

$$\sigma_w^2 = \frac{(NT)^2}{12} \tag{34}$$

are the variances that have been chosen to match those of the rectangular-shaped signals. The multiplicative factors in Equations (29), (30), and (31) are chosen such that the areas under the Gaussian signals match those of the rectangular signals.

From Equation (16) we have learned that to compute the filter output $\overline{S}_{mf}$, we need to compute the cross correlation of $s(x)$ and $s_F(x)$. For Gaussian signals, this is given by

$$R_{s,s_F}(x) = \frac{12\sigma_T\sigma_F}{\sqrt{2\pi(\sigma_T^2+\sigma_F^2)}} \exp\left[-\frac{x^2}{2(\sigma_T^2+\sigma_F^2)}\right] \quad . \tag{35}$$

Therefore, $\overline{S}_{mf}$ is

$$\begin{aligned}\overline{S}_{mf} &= \frac{\lambda_s}{\Delta v}\int_R w\left(\frac{x}{N\Delta vT}\right)R_{s,s_F}(x)dx \\ &= \lambda_s\sqrt{\frac{6}{\pi}}\frac{12\sigma_T\sigma_F\sigma_w}{\sqrt{\sigma_T^2+\sigma_F^2+\Delta v^2\sigma_w^2}}\end{aligned} \tag{36}$$

and the noise variance at the filter output is

$$\sigma_{0,mf}^2 = \lambda_0\int w^2(\eta)d\eta\int s_F^2(\xi)d\xi = \frac{36\lambda_0}{\pi}\sigma_w\sigma_F \quad . \tag{37}$$

Using Equation (36) and (37), it is easy to see that

$$\begin{aligned}\frac{\mathrm{SNR}_{out}}{\mathrm{SNR}_{in}} &= \frac{24\sigma_T^2\sigma_F\sigma_w}{\sigma_T^2+\sigma_F^2+\Delta v^2\sigma_w^2} \\ &= \frac{\mathrm{SNR}_{out}}{\mathrm{SNR}_{in}}\Big|_{\Delta v=0}\frac{2v_F/v_T}{1+v_F^2/v_T^2+N^2(v_F-v_T)^2/v_T^2} \quad .\end{aligned} \tag{38}$$

Letting $\chi = v_F/v_T$ and

$$\rho \equiv \frac{2v_F/v_T}{1+v_F^2/v_T^2+N^2(v_F-v_T)^2/v_T^2} \tag{39}$$

we obtain the following quadratic equation

$$\chi^2 - \frac{2N^2+2/\rho}{N^2+1}\chi + 1 = 0 \quad . \tag{40}$$

A useful solution of Equation (40) is given by

$$\chi \equiv \frac{v_F}{v_T} = \frac{1}{N^2+1}\left[N^2+\frac{1}{\rho}-\sqrt{2\left(\frac{1}{\rho}-1\right)N^2+\left(\frac{1}{\rho^2}-1\right)}\right] \quad . \tag{41}$$

Similar to Figures 3 and 4, we have plotted Figures 5 and 6 for the Gaussian-shaped signal, using Equation (41).

By examining the equations and the figures, we conclude that the Gaussian approximation renders the same filter characteristics as the original rectangular signals, i.e., the spacing between filter velocities increases as the expected target velocity increases. Owing

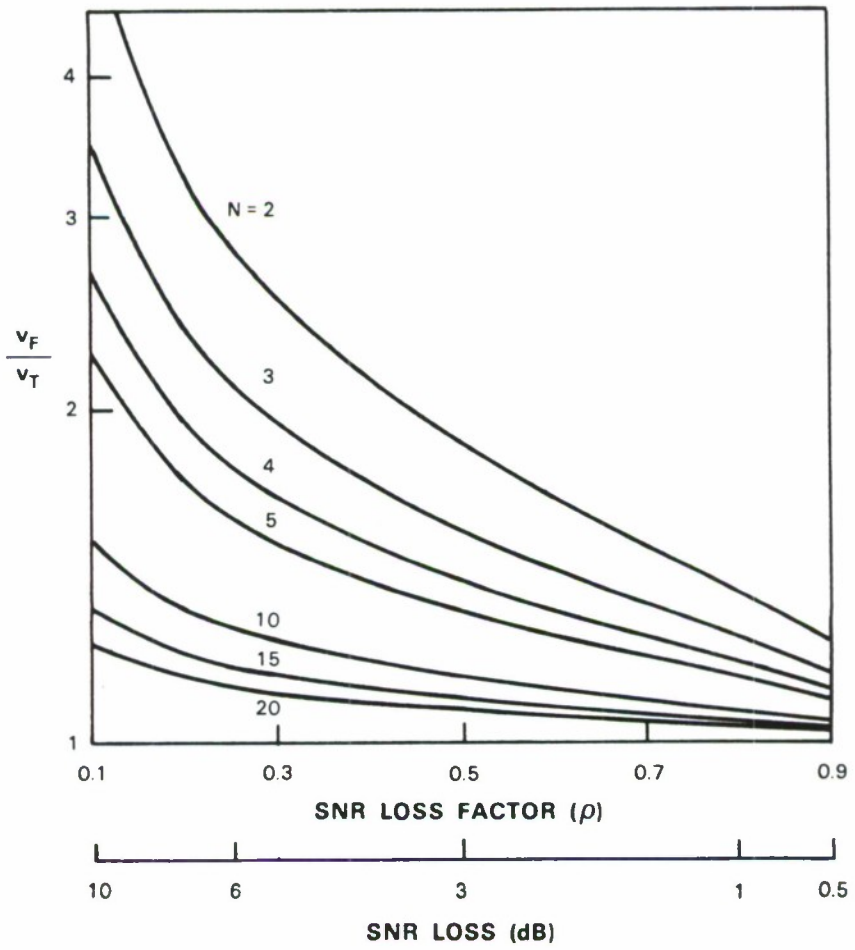

Figure 5. v_F/v_T – Gaussian signal.

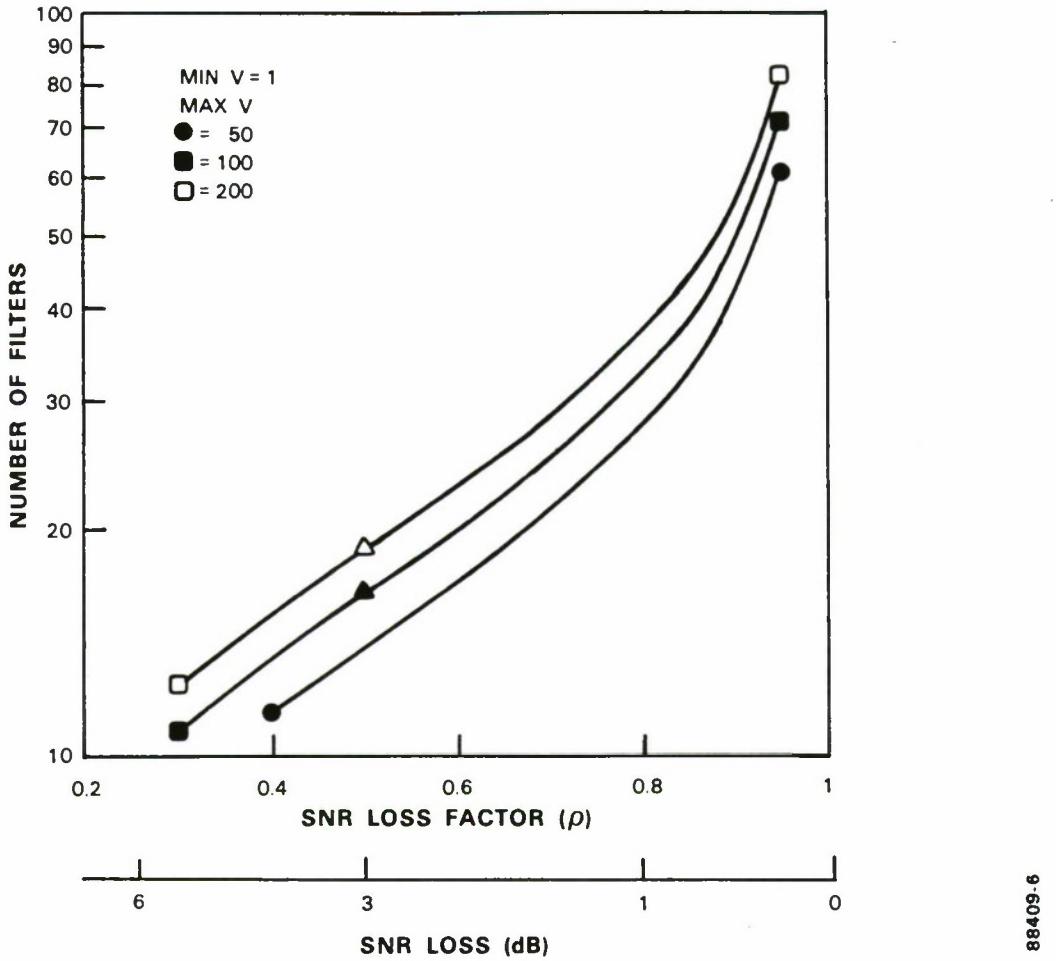

Figure 6. Number of filters required – Gaussian signal.

to its mathematical tractability, we will use the Gaussian approximation in designing the two-dimensional AVF.

3 THE DESIGN OF THE TWO-DIMENSIONAL AVF

Two-dimensional assumed velocity filtering may have mismatches either in the speed or direction of movement. In this section, we use the Gaussian-shaped signals for the investigation of SNR loss due to such mismatches. Finally, we will use the results to partition a two-dimensional target velocity space.

Without loss of generality, we assume that the target signal, described by length $v_T T$ and width h, is aligned with the horizontal axis. The filter signal, with length $v_F T$ and width h, intersects the target signal at an angle θ. In the Gaussian signals, we define σ_T^2 and σ_F^2 as in Equations (32) and (33). In addition, to approximate the signal width we use a variance

$$\sigma_h^2 = h^2/12 \quad . \tag{42}$$

Now the target and filter signals are given by

$$s(\underline{x}) = \frac{6}{\pi} \exp\left(-\frac{1}{2}\underline{x}^t K_T^{-1} \underline{x}\right) \tag{43}$$

$$s_F(\underline{x}) = \frac{6}{\pi} \exp\left(-\frac{1}{2}\underline{x}^t K_F^{-1} \underline{x}\right) \tag{44}$$

where $\underline{x}^t = [x_1 \; x_2]$. The covariance matrix of the target signal, K_T, is the diagonal matrix

$$K_T = \begin{bmatrix} \sigma_T^2 & 0 \\ 0 & \sigma_h^2 \end{bmatrix} \quad . \tag{45}$$

The covariance matrix of the filter signal, K_F, is another diagonal matrix rotated by a

similarity transformation

$$K_F = \begin{bmatrix} \cos\theta & \sin\theta \\ -\sin\theta & \cos\theta \end{bmatrix} \begin{bmatrix} \sigma_F^2 & 0 \\ 0 & \sigma_h^2 \end{bmatrix} \begin{bmatrix} \cos\theta & -\sin\theta \\ \sin\theta & \cos\theta \end{bmatrix}$$

$$= \begin{bmatrix} \sigma_F^2 \cos^2\theta + \sigma_h^2 \sin^2\theta & (\sigma_h^2 - \sigma_F^2)\sin\theta\cos\theta \\ (\sigma_h^2 - \sigma_F^2)\sin\theta\cos\theta & \sigma_F^2 \sin^2\theta + \sigma_h^2 \cos^2\theta \end{bmatrix} . \quad (46)$$

The cross correlation of $s(\underline{x})$ and $s_F(\underline{x})$ is given by

$$R_{s,s_F}(\underline{x}) = \frac{72\sqrt{|K_T||K_F|}}{\pi\sqrt{|K_T + K_F|}} \exp\left[-\frac{1}{2}\underline{x}^t(K_T + K_F)^{-1}\underline{x}\right] . \quad (47)$$

Using Equation (47) and the temporal weighting function, we can compute the output signal $\overline{S}_{mf}$ and the noise variance as

$$\begin{aligned} \overline{S}_{mf} &= \lambda_s \int w(t) R_{s,s_F}(\Delta\underline{v}t)dt \\ &= \frac{72\sqrt{12|K_T||K_F|}\lambda_s}{\pi\sqrt{|K_T + K_F|[1/\sigma_w^2 + \Delta\underline{v}^t(K_T + K_F)^{-1}\Delta\underline{v}]}} \quad (48) \\ \sigma_{0,mf}^2 &= \lambda_0 \int w^2(\underline{\eta})d\underline{\eta} \int s_F^2(\underline{\xi})d\underline{\xi} \\ &= \frac{432\sigma_w\lambda_0}{\sqrt{2\pi}\pi}\sqrt{|K_F|} \quad (49) \end{aligned}$$

where

$$\Delta\underline{v} = \begin{bmatrix} v_F\cos\theta - v_T \\ \\ v_F\sin\theta \end{bmatrix} . \quad (50)$$

Using the above equations, we can express SNR_{out} as

$$\begin{aligned} \mathrm{SNR}_{out} &= 144\sqrt{\frac{2}{\pi}} \frac{|K_T||K_F|\lambda_s^2}{|K_T + K_F|\sqrt{|K_F|}\sigma_w[1/\sigma_w^2 + \Delta\underline{v}^t(K_T + K_F)^{-1}\Delta\underline{v}]\lambda_0} \\ &= 144\sqrt{\frac{2}{\pi}} \frac{|K_T||K_F|\ \mathrm{SNR}_{in}}{|K_T + K_F|\sqrt{|K_F|}\sigma_w[1/\sigma_w^2 + \Delta\underline{v}^t(K_T + K_F)^{-1}\Delta\underline{v}]} . \quad (51) \end{aligned}$$

Therefore, we can write the following equation for the description of the average loss of

SNR due to the velocity mismatch

$$\frac{\mathrm{SNR}_{out}}{\mathrm{SNR}_{in}} = \frac{\mathrm{SNR}_{out}}{\mathrm{SNR}_{in}}\Big|_{\Delta \underline{v}=0} \frac{4\sqrt{|K_T||K_F|}}{|K_T+K_F|\sigma_w^2[1/\sigma_w^2 + \Delta \underline{v}^t (K_T+K_F)^{-1}\Delta \underline{v}]} \quad . \tag{52}$$

Now let

$$\rho \equiv \frac{4\sqrt{|K_T||K_F|}}{|K_T+K_F|\sigma_w^2[1/\sigma_w^2 + \Delta \underline{v}^t (K_T+K_F)^{-1}\Delta \underline{v}]} \quad . \tag{53}$$

It can be verified that

$$\sqrt{|K_T||K_F|} = \sigma_T \sigma_F \sigma_h^2 \tag{54}$$

$$\begin{aligned} |K_T+K_F| &= \sigma_T^2\sigma_h^2 + \sigma_F^2\sigma_h^2 + \sigma_T^2\sigma_F^2 \sin^2\theta + \sigma_T^2\sigma_h^2\cos^2\theta \\ &\quad + \sigma_F^2\sigma_h^2\cos^2\theta + \sigma_h^4 \sin^2\theta \end{aligned} \tag{55}$$

$$\begin{aligned} (K_F+K_T)^{-1} &= \frac{1}{(\sigma_T^2+\sigma_F^2)\sigma_h^2(1+\cos^2\theta) + (\sigma_T^2\sigma_F^2+\sigma_h^4)\sin^2\theta} \\ &\quad \cdot \begin{bmatrix} \sigma_F^2\sin^2\theta + \sigma_h^2(1+\cos^2\theta) & (\sigma_F^2-\sigma_h^2)\sin\theta\cos\theta \\ (\sigma_F^2-\sigma_h^2)\sin\theta\cos\theta & \sigma_T^2+\sigma_F^2\cos^2\theta + \sigma_h^2\sin^2\theta \end{bmatrix} \quad . \end{aligned} \tag{56}$$

Using Equations (50), (54), (55), and (56), and letting $\chi \equiv v_F/v_T$ and $\alpha \equiv h^2/v_T^2T^2$ Equation (53) can be rewritten as a quartic equation in χ

$$\begin{aligned} &(4\rho N^2 \sin^2\theta\cos^2\theta)\chi^4 - (4\rho N^2\sin^2\theta\cos\theta)\chi^3 \\ &+[\rho\alpha(1+\cos^2\theta) + \rho\sin^2\theta + 2\rho N^2\sin^2\theta + \rho N^2\alpha(1+\cos^2)\cos^2\theta - 2\rho N^2\alpha\sin^2\theta\cos^2\theta \\ &-2\rho N^2\alpha\sin^2\theta\cos^2\theta + \rho N^2\alpha\sin^4\theta]\chi^2 \\ &+[-4\alpha - 2\rho N^2\alpha(1+\cos^2\theta)\cos\theta + 2\rho N^2\alpha\sin^2\theta\cos\theta]\chi \\ &+[\rho\alpha(1+\cos^2\theta) + \rho\alpha^2\sin^2\theta + \rho N^2\alpha(1+\cos^2\theta)] \\ &= 0 \quad . \end{aligned} \tag{57}$$

Equation (57) can be solved for a given set of θ (see footnote). The results may be used to partition the $v - \theta$ plane. Keeping $N = 10$, we plot the filter 3-dB loss contours in Figure 7 for a set of carefully spaced filters. A target with speed and angle contained in any of the cells will be detected by the corresponding filter with an SNR loss ≤ 3 dB. Because of the irregular shape of the cells, proper overlapping will be required to fill the gaps. For clarity, we do not show such overlapping in this and all subsequent figures.

The design of the suboptimal two-dimensional AVF amounts to the partitioning of the velocity space using Equation (57). As an example, we have designed filters with a maximum 3-dB loss for the coverage of the $v_1 - v_2$ plane, where $1 < \sqrt{v_1^2 + v_2^2} < 10$. The partitioning of the velocity space is shown in Figure 8(a). A very useful property of the design can be noticed in the figure, that is, the radial spreading of the resolution cells. Had the size of the cells remained unchanged, the number of filters required for coverage would have increased quadratically as v_1 and v_2 increased. However, due to the radial spreading of the cell size, we expect this growth to be much slower. A count of the number of filters (less those overlapping), shows a linear growth rate, as indicated in Figure 8(b). This property is crucial for making efficient implementation of AVFs feasible.

Two situations may occur in solving Equation (57):

1. There are no real solutions. For the given θ, the loss factor ρ cannot be satisfied.
2. There is one and only one pair of real solutions. The real solutions are the solutions of interest.

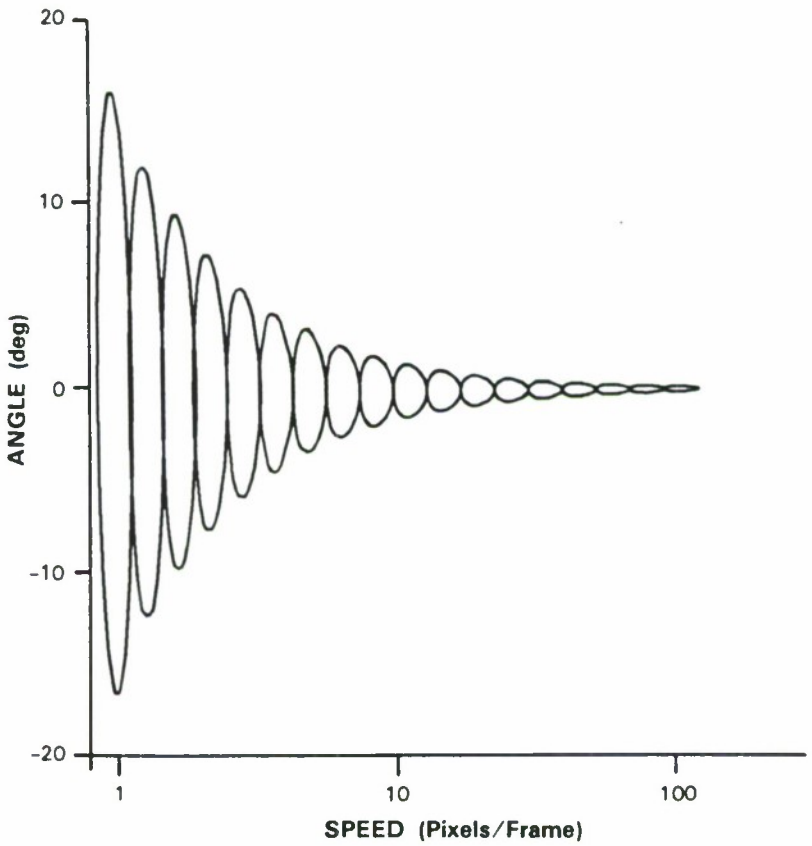

88409-7

Figure 7. Filter 3-dB contours in speed–angle space.

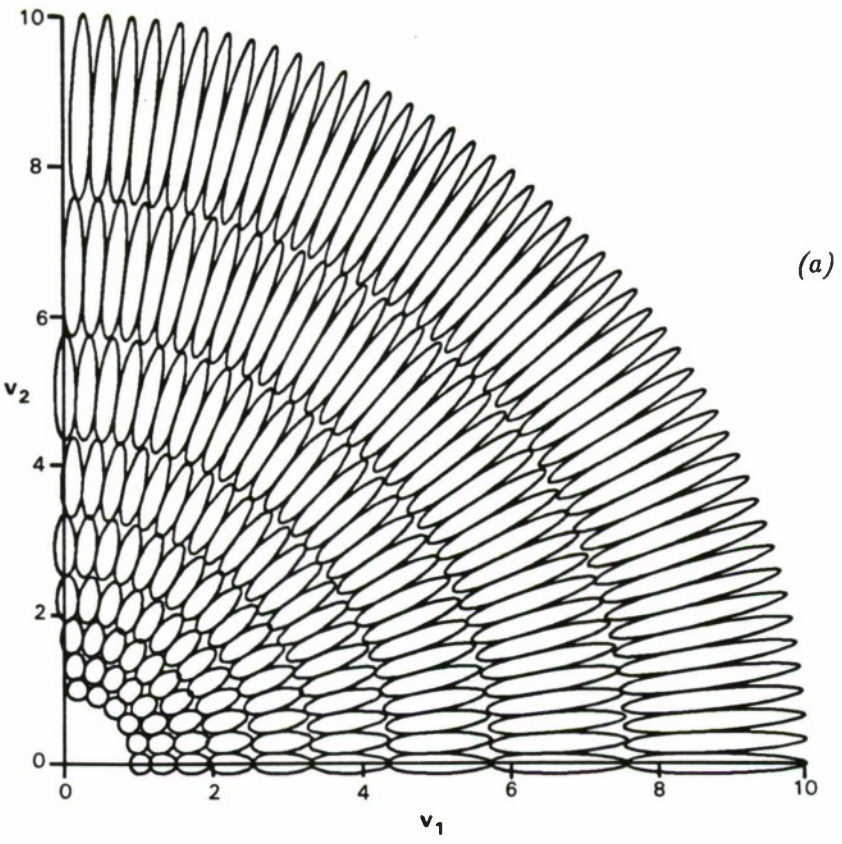

(a)

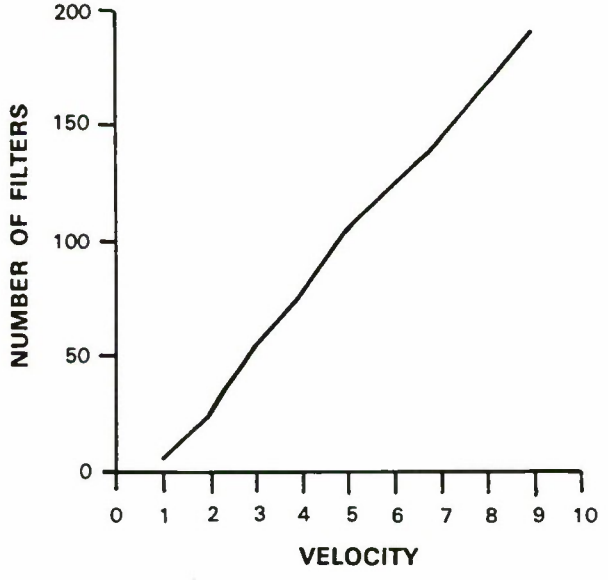

(b)

Figure 8. Fixed loss factor. (a) placement and (b) growth rate of filters.

4 THE VARIABLE LOSS FACTOR

In the begining of this section, we take a slight change of course and investigate how the filter-output SNR_{out}, varies as a function of target speed. Later, we will return to the topic of AVF design and we will use the result developed to define a variable loss factor, as opposed to the previously used fixed loss factor. Through the same example of the last section, we will demonstrate that even greater efficiency can be achieved with the variable loss factor.

Assuming a perfectly matched filter, Equation (51) can be simplified to

$$\mathrm{SNR}_{out}|_{\Delta_{\underline{v}}=0} = 6\sqrt{\frac{6}{\pi}}\frac{\lambda_s^2\sigma_h\sigma_w v_T T}{\lambda_0} \quad . \tag{58}$$

The SNR_{out} is seen to be proportional to v_T, a well-known characteristic of matched filtering. Hidden in Equation (58) is that SNR_{out} may also be related to v_T through its association with λ_s, the electron rate due to the target signal. The λ_s is inversely proportional to both the target angular speed and the square of the distance between the sensor and the target. Let r be this distance, then

$$\lambda_s = \frac{C}{v_T r^2} \tag{59}$$

where C, the constant of proportionality, accounts for the visual magnitude of the sun, effective cross section of the target, frame integration time, telescope aperture, CCD photon efficiency, etc.

Based on Equation (59) we will treat three different cases of ground-based sensors:

Case 1. The sensor is located at the center of the earth [as shown in Figure 9(a)]. By Kepler's third law

$$\theta \equiv v_T T \propto r^{-3/2} \quad . \tag{60}$$

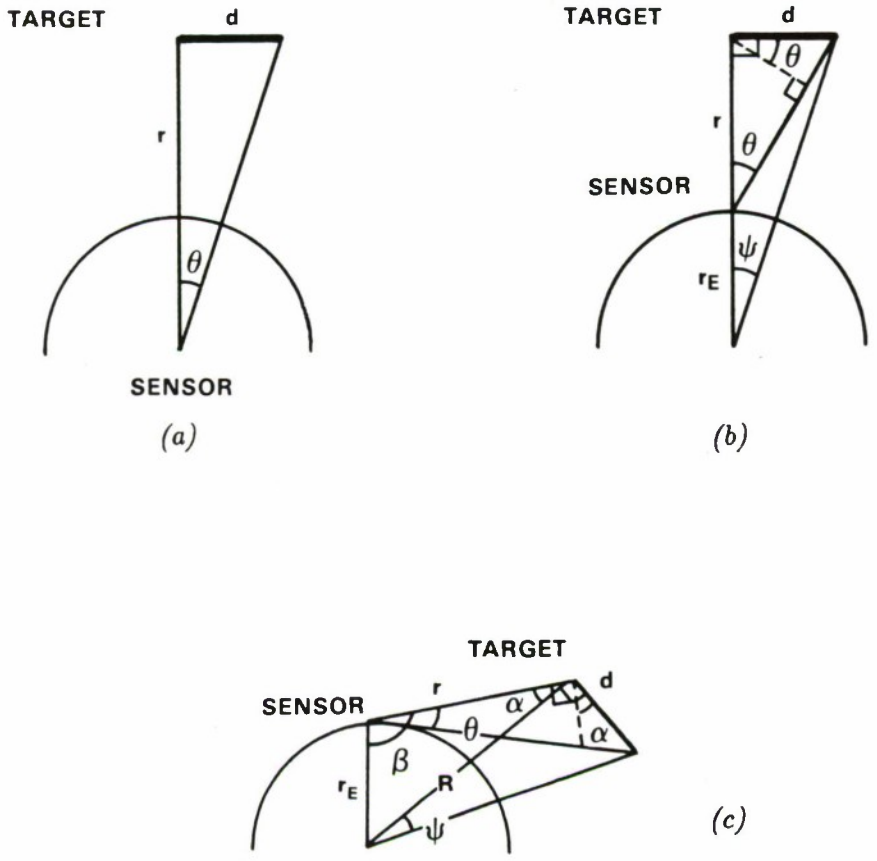

Figure 9. Sensor–target geometry.

Substituting Equation (60) into (59) yields

$$\lambda_s \propto v_T^{1/3} \quad . \tag{61}$$

Finally, substituting Equation (61) back into (58) yields

$$\mathrm{SNR}_{out} \propto v_T^{5/3} \quad . \tag{62}$$

Case 2. The sensor is located on the surface of the earth and the target is directly overhead [as shown in Figure 9(b)]. For simplicity, we ignore the rotation of the earth. From the figure, Kepler's third law is stated as

$$\psi \propto (r + r_E)^{-3/2} \tag{63}$$

where r_E is the local radius of the earth. Since

$$\psi \approx d\,(r + r_E)^{-1} \tag{64}$$

the linear velocity d relates to r through

$$d \propto (r + r_E)^{-1/2} \tag{65}$$

and then the angular velocity v_T relates to r through

$$\begin{aligned} \theta &\equiv v_T T \propto r^{-1}(r + r_E)^{-1/2} \cos\theta \\ &\approx r^{-1}(r + r_E)^{-1/2} \end{aligned} \tag{66}$$

where we have assumed that the angle θ is small. We consider the following two extremes:

I. When $r \gg r_E$, then

$$v_T \propto r^{-3/2} \quad . \tag{67}$$

Since Equation (67) is identical to (60) in Case 1, we conclude that Equation (62) holds in this case too.

II. When $r \ll r_E$, then

$$v_T \propto r^{-1} \quad . \tag{68}$$

Substituting Equation (68) into (59) yields

$$\lambda_s \propto v_T \quad . \tag{69}$$

That is, λ_s increases as the angular target speed increases. Therefore, in this case

$$\mathrm{SNR}_{out} \propto v_T^3 \quad . \tag{70}$$

Case 3. The sensor is located on the surface of the earth. The target, sensor, and center of the earth form an angle β [as shown in Figure 9(c)]. This is a generalization of Case 2. Applying Kepler's third law again we have

$$\psi \propto R^{-3/2} \tag{71}$$

$$d \propto R^{-1/2} \tag{72}$$

and

$$\theta \equiv v_T T \propto r^{-1} R^{-1/2} \cos\alpha \quad . \tag{73}$$

By the law of cosines we can find $\cos\alpha$. It is given by

$$\cos\alpha = (r - r_E \cos\beta) R^{-1} \quad . \tag{74}$$

Substituting Equation (74) into (73) yields

$$\theta \equiv v_T T \propto r^{-1}(r^2 + r_E^2 - 2 r r_E \cos\beta)^{-3/4}(r - r_E \cos\beta) \quad . \tag{75}$$

Now it can be verified easily that the two extremes of Case 2 hold approximately true even when the target is not directly overhead.

In all three cases of ground-based sensors, we have shown that SNR_{out} is at least proportional to $v_T^{5/3}$. The implication of the above relationships is that fast targets are brighter and therefore they are easier to detect (greater probability of detection at the same probability of false alarm) than slow targets. For the purpose of efficient utilization of detector resources, it may be desirable to design a detector with uniform sensitivity to various target speeds. This can be achieved through adjusting the loss factor in anticipation of different expected target angular speed.

To demonstrate, we will adopt a conservative linear relationship. Let v_0 be the lowest angular speed the system is designed to detect; let $v \geq v_0$ be that of an arbitrary target; and let

$$\rho' = \left(\frac{v}{v_0}\right)^{-1} \rho \quad . \tag{76}$$

Letting $v_0 = 1$, we rework the example in the last section. The loss factor ρ' is now $1/2v$ for $\rho = 1/2$. The partitioning of the velocity space, based on the solutions of Equation (57), is plotted in Figure 10(a). Notice that the size of the resolution cells increases quite dramatically compared with that of Figure 8(a). Figure 10(b) illustrates the much slower growth rate demonstrated in this example. For comparison, 38 filters are needed to cover the 10 pixels per frame velocity space (with no overlapping of cells) in this example, whereas 191 filters were needed when the loss factor was held constant.

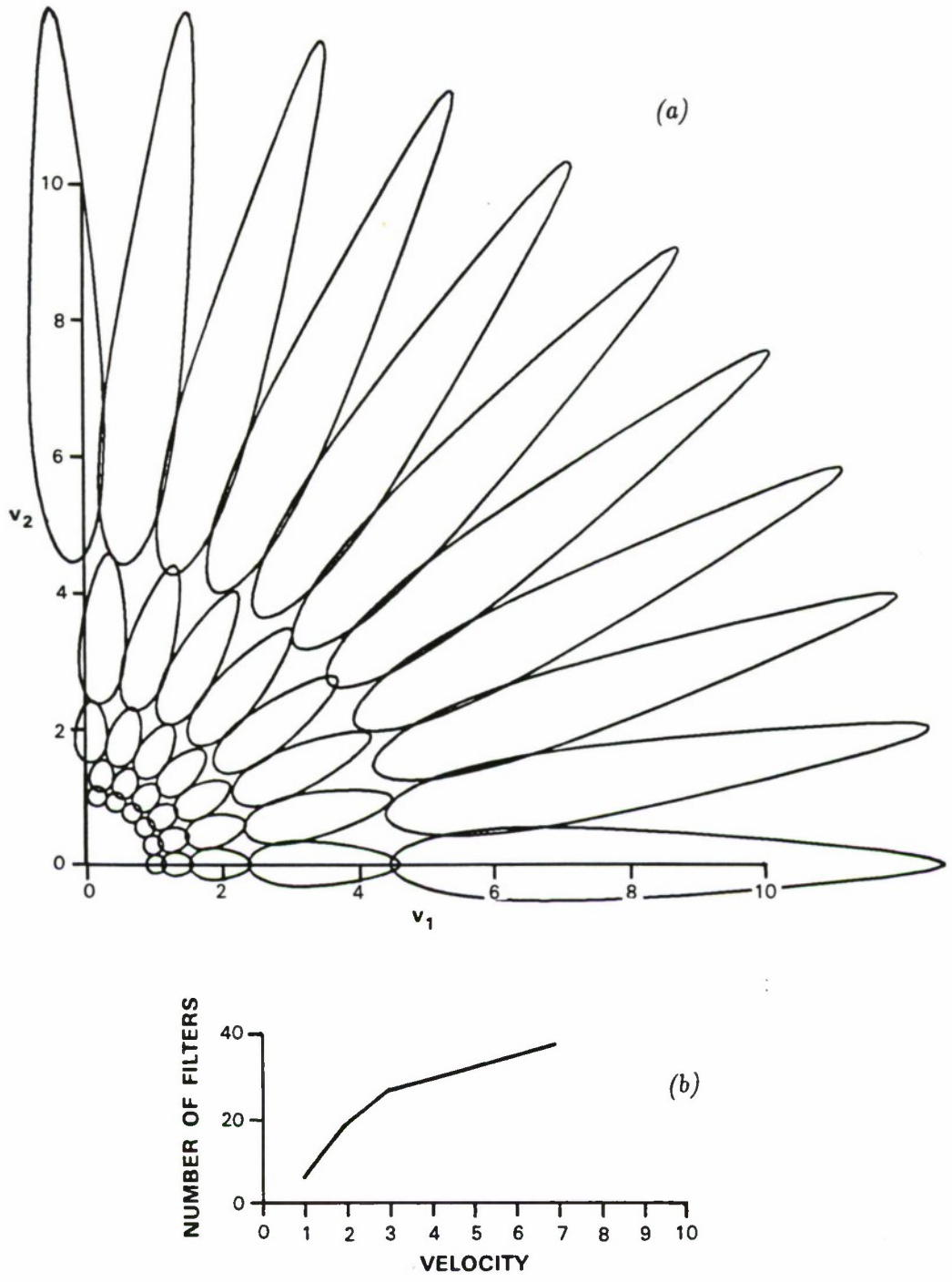

Figure 10. *Variable loss factor. (a) placement and (b) growth rate of filters.*

5 SUMMARY

The problem of matched-filter detection of three-dimensional moving targets is considered. Both the signal and noise are assumed to be Poisson processes. The matched filters are derived based on a weak signal model. They are called the assumed-velocity filters (AVFs) because velocity is the only filter parameter. For efficient implementation of the AVF it is necessary to partition the velocity space. For this purpose, we have introduced a loss factor which characterizes the loss of SNR due to velocity mismatches. For a prescribed maximum loss, we have derived mathematical equations that can be used to compute the boundary of velocity resolution cells. The cells can then be used to partition velocity space. We have shown, through simulation, that the number of matched filters required increases linearly as the span of the velocity space increases — a desirable property. Finally, we discussed the use of the variable loss factor where we have explored the increase in signal intensity due to the closeness of a target. Using the variable loss factor, the number of filters required for coverage is further reduced to only a few dozen for single quadrant coverage.

ACKNOWLEDGMENT

The author would like to thank Dr. A. E. Filip of MIT Lincoln Laboratory for his many enlightening discussions.

REFERENCES

1. I. S. Reed, R. M. Gagliardi, and H. M. Shao, "Application of Three-Dimensional Filtering to Moving Target Detection," IEEE Trans. Aerosp. Electron. Syst., **AES-19**, 898 (1983).

2. N. C. Mohanty, "Computer Tracking of Moving Point Target in Space," IEEE Trans. Pattern Anal. Mach. Intell., **PAMI-3**, 606 (1981).

3. S. C. Pohlig, MIT Lincoln Laboratory, "An Algorithm for Detection of Moving Optical Targets," to be published.

UNCLASSIFIED

SECURITY CLASSIFICATION OF THIS PAGE

REPORT DOCUMENTATION PAGE

1a. REPORT SECURITY CLASSIFICATION Unclassified	1b. RESTRICTIVE MARKINGS
2a. SECURITY CLASSIFICATION AUTHORITY	3. DISTRIBUTION/AVAILABILITY OF REPORT Approved for public release; distribution unlimited.
2b. DECLASSIFICATION/DOWNGRADING SCHEDULE	
4. PERFORMING ORGANIZATION REPORT NUMBER(S) TR-795	5. MONITORING ORGANIZATION REPORT NUMBER(S) ESD-TR-87-093
6a. NAME OF PERFORMING ORGANIZATION Lincoln Laboratory, MIT 6b. OFFICE SYMBOL *(If applicable)*	7a. NAME OF MONITORING ORGANIZATION Electronic Systems Division
6c. ADDRESS *(City, State, and Zip Code)* P.O. Box 73 Lexington, MA 02173-0073	7b. ADDRESS *(City, State, and Zip Code)* Hanscom AFB, MA 01731
8a. NAME OF FUNDING/SPONSORING ORGANIZATION Air Force Systems Command, USAF 8b. OFFICE SYMBOL *(If applicable)* AFSTC	9. PROCUREMENT INSTRUMENT IDENTIFICATION NUMBER F19628-86-C-0002
8c. ADDRESS *(City, State, and Zip Code)* Kirtland Air Force Base NM 87117-6005	10. SOURCE OF FUNDING NUMBERS PROGRAM ELEMENT NO.: 63220C PROJECT NO.: 287 TASK NO.: WORK UNIT ACCESSION NO.:

11. TITLE *(Include Security Classification)*

On the Design of Suboptimal Matched Filters for Three-Dimensional Moving Target Detectors

12. PERSONAL AUTHOR(S)
Yeunung Chen

13a. TYPE OF REPORT	13b. TIME COVERED	14. DATE OF REPORT *(Year, Month, Day)*	15. PAGE COUNT
Technical Report	FROM _____ TO _____	1987 November 20	40

16. SUPPLEMENTARY NOTATION
None

17. COSATI CODES			18. SUBJECT TERMS *(Continue on reverse if necessary and identify by block number)*
FIELD	GROUP	SUB-GROUP	moving target detection; assumed velocity filtering; matched filtering; Poisson distribution; maximum-likelihood detection; SNR loss factor; CCD photodetector; variable SNR loss factor

19. ABSTRACT *(Continue on reverse if necessary and identify by block number)*

The optimal detection of a three-dimensional moving target calls for the classical technique of matched filtering. If a target is modeled as a moving point source with unknown velocity, then the velocity alone determines the shape of the observed signal. Thus, target velocity is a parameter that completely characterizes the matched filter. We will designate these types of matched filters to be the assumed velocity filters (AVF) to emphasize the velocity parameter.

Like most matched filtering techniques where the signal parameters range in a continuum, the AVF must be implemented suboptimally by quantizing the velocity space. In this report we will use a loss factor that measures the average loss of signal-to-noise ratio (SNR) at the output of the matched filter due to mismatch of filter parameters. The loss factor can be used as a criterion for partitioning the velocity space. We will show that, with a fixed loss factor, the number of filters required for coverage increases *linearly* as the span of the two-dimensional velocity space increases quadratically. The rate of increase is further reduced when the loss factor is made proportional to expected target angular speed.

20. DISTRIBUTION/AVAILABILITY OF ABSTRACT	21. ABSTRACT SECURITY CLASSIFICATION
☐ UNCLASSIFIED/UNLIMITED ☒ SAME AS RPT. ☐ DTIC USERS	Unclassified
22a. NAME OF RESPONSIBLE INDIVIDUAL Hugh L. Southall, Lt. Col., USAF	22b. TELEPHONE *(Include Area Code)* (617) 863-5500, Ext. 2330 22c. OFFICE SYMBOL ESD/TML

DD FORM 1473, 84 MAR 83 APR edition may be used until exhausted. All other editions are obsolete.

UNCLASSIFIED

SECURITY CLASSIFICATION OF THIS PAGE